FERROGEL-BASED WIRELESS ACOUSTO-BIOCHEMICAL SENSING

Jiseon Lee[1], Chaerin Jun[1], Eungyoul Oh[1], Jeonga Han[1], Albert Kim[2] and Seunghyun Song[1]
[1]Department of Electronics Engineering, Sookmyung Women's University, Seoul, SOUTH KOREA
[2]Temple University, Philadelphia, PA, USA

2021 21st International Conference on Solid-State Sensors, Actuators and Microsystems (Transducers) | 978-1-6654-1267-4/21/$31.00 ©2021 IEEE | DOI: 10.1109/TRANSDUCERS50396.2021.9495583

ABSTRACT

Continuous monitoring of biochemical information is critical for health management. Hydrogel, a synthetic material that exhibits volumetric response to target stimuli, is an attractive material for such applications. However, wireless readout of the hydrogel's response over a longer distance, while maintaining the small sensor dimension has been challenging. In this work we present ferrogel-based wireless acousto-biochemical sensing system with small dimension (length: 7.5 mm, diameter: 2 mm) and long sensing distance (>10 cm). The sensor utilizes ferromagnetic hydrogel to convert pH to the change in resonance frequency; the wireless measurement is made through the RF signal emission under ultrasonic excitation.

KEYWORDS

Hydrogel, pH sensor, wireless biochemical sensor, ultrasound

INTRODUCTION

Human's biochemistry is highly regulated and thus the imbalances of the biochemical parameters (such as glucose levels, local pH, stress hormone levels, and more) are important biomarkers for identifying conditions [1]. One methodological approach is to use an implantable sensor for continuous monitoring of biochemical information that includes biochemical transduction components [2]. Enzymes, antibodies, receptors, or nucleic acids are commonly utilized for biochemical sensors; however, for an implantable device, the limited activity duration of the abovementioned materials becomes an issue as the sensors cannot be frequently replaced/replenished [3], [4].

From this perspective, hydrogels, highly hygroscopic polymeric networks, is an attractive alternative material for biochemical transduction as they can be engineered to be sensitive to different biochemical stimuli such as pH [5], [6], glucose [4], [7], cortisol [8], tumor necrosis factor [3] and etc [1]. Moreover, they are protein-free and purely synthetic and thus can potentially be used for a long-term implantation [4]. These advantages have prompted many researchers to develop hydrogel based sensors and smart systems [3]–[7]. However, the telemetry of the hydrogel's volumetric response to the external readout system has mostly been limited to passive LC transponder scheme whose working distance only spans around 1 cm.

In this work, we propose a ferrogel-based wireless acousto-biochemical sensing system and demonstrate wireless pH measurement using the prototype device; the sensor employs ferrogel (hydrogel embedded with ferromagnetic particles) as the actuation source for the movable ferrite core. The on-board ultrasonic energy harvester converts the incoming ultrasound to electrical energy, which triggers the LC transponder to emit RF (radio frequency) signals.

RESULTS & DISCUSSIONS

Ferrogel-Based Wireless Acousto-Biochemical Sensor Design

The prototype ferrogel-based wireless acousto-biochemical sensor operation is illustrated in Fig. 1. The sensor converts the incoming ultrasonic waves to RF signal, which contains the frequency component corresponding to the resonance frequency of the LC transponder. The LC transponder is capable of pH sensing through pH sensitive acrylamide-based hydrogel embedded with ferromagnetic particles (ferrogel). The inclusion of the ferromagnetic particles enables the ferrogel to be attached to a ferrite rod by a magnet. The pH sensitive hydrogel used in our study is acrylamide-co-methacrylic acid hydrogel; the pK_a of methacrylic acid is around 4.8, hence the carboxyl groups ionize in basic pH, resulting in electrostatic repulsion between the chains and the hydrogel expansion. The volumetric response to the pH of the ferrogel is then translated to the displacement of the ferrite rod, which modulates the inductance of the solenoid and hence the resonant frequency of the LC transponder.

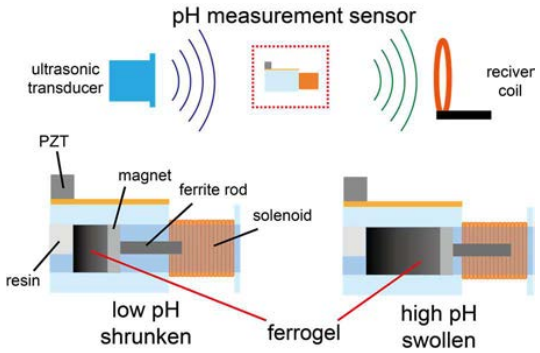

Figure 1. Schematic illustration of the ferrogel-based wireless acousto-biochemical sensor

Ferrogel Synthesis and Device Fabrication

The device fabrication process is outlined in Fig. 2a-e. Firstly, the recipe for the ferrogel synthesis is based on previous publications [5], [6]. Briefly, we added 2.8 g of acrylamide, 830 µl of N,N,N',N'- tetramethyl-ethylenediamine, 840 µl of methacrylic acid, and 136 mg of N, N'-methylenebisacrylamide to 10 ml of DI water (all reagents were purchased from Sigma Aldrich, USA), followed by the addition of 1.5 g of iron (II, III) oxide (Daejung Chemical, South Korea). The initiator solution was prepared by dissolving 80 mg/ml ammonium persulfate (Daejung Chemical, South Korea). The pregel solution and the initiator solution were mixed in a 6:1 ratio to form the ferrogel (Fig. 2a). The mixed solution was then poured into a polycarbonate petri dish and left to polymerize for 10 minutes (Fig. 2b). After polymerization, we equilibrated the ferrogel in pH 4 solution; afterwards we cored out the cured ferrogel using a 1.5 mm diameter

biopsy punch as shown in Fig. 2c (Ted Pella, USA). Fig. 2d shows the microscope image (Leica MZ10F) of the ferrogel core.

The exploded view of the sensor is shown in Fig. 2e. To assemble the sensor, we firstly prepared a 3D printed shell that is 7.5 mm in length and 2.1 mm outer diameter and 1.4 mm inner diameter. The cladded copper wire was then wrapped around the cylinder to form a solenoid. Into the solenoid, we inserted an assembly of ferrogel-magnet-ferrite rod (Fig. 2f). The magnetic force holds together the assembly together. Finally, the end of the cylindrical shell is half-sealed with a UV curable resin to prevent ferrogel leakage without completely inhibiting solution exchange (Fig. 2g). The 3D printed shell also has pores (diameter of 350 μm) on the side to further facilitate the solution diffusion into the ferrogel to improve both sensitivity and the response time of the sensor (Fig. 2h). The photograph of the sensor is shown in Fig. 2i.

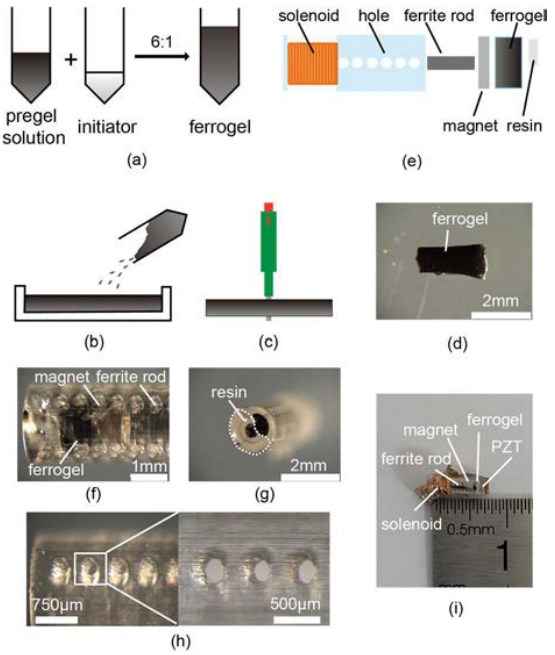

Figure 2. Ferrogel synthesis and sensor fabrication. (a) Ferrogel synthesis (b) Curing ferrogel in a mold (c) Coring out ferrogel cylinder (d) Microscope image of the ferrogel core (e) Exploded-view of the sensor assembly (f) microscope image of the ferrogel-magnet-ferrite rod assembly in the cylindrical shell. (g) The side view image of the sensor with the resin covering half of the cylinder end. (h) microscope image of the pores with a diameter of 350 μm. (i) photograph of the assembled sensor.

Ferrogel Swelling Behavior Characterization

The inclusion of the ferromagnetic particles to the pH sensitive hydrogel is what enables the magnetic force to hold the core assembly of ferrogel, magnet, and ferrite rod together; thus, the concentration of the ferromagnetic particles should be sufficiently high for the ferrogel to remain attached to the magnet throughout volume expansion/reduction. Meanwhile, the excessive ferromagnetic particle concentration can lead to leaching and deterioration of the volumetric response.

The experimentally determined value for the optimal ferromagnetic particle concentration was 15 w/v percentage, where the magnetic interaction is strong enough without adversely affecting the swelling behavior. Fig. 3a-d show the microscope images of the ferrogel cylinder (initial dimension of 2.6 mm in length and 1.5 mm in diameter). The ferrogel dimensions exhibited isotropic swelling behavior, which was fitted with a Boltzmann's sigmoidal equation (red line) with the transition pH of 6 and a swelling ratio of 1.7 (the swelling ratio is consistent with the previous reports [5]). However, we observed a discrepancy between transition pH of the ferrogel and the ionization pH of the methacrylic acid group (pK_a = 4.8), which drives the swelling of pH sensitive hydrogel through the increased electrostatic repulsion between ironized groups. We tentatively assign this to the inclusion of the iron (II, III) oxide particles interacting with the ionized group and perhaps an increased electrostatic screening effects of the charged particles, which will require a further investigation. Nevertheless, we experimentally confirmed that the inclusion of 15 w/v% of iron (II, III) oxide does not decrease the swelling ratio for hydrogel.

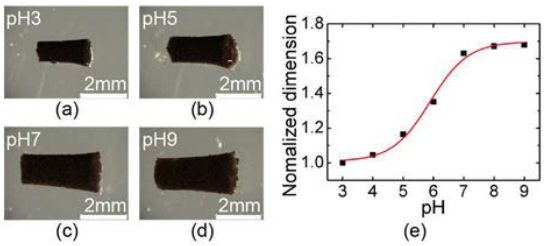

Figure 3. Swelling behavior of the ferrogel. (a-d) Microscope images of the ferrogel cylinder in different pH solutions (e) Free swelling curve of the uncaged ferrogel.

Subsequently, we characterized the swelling behavior of the ferrogel inside of the cylindrical tube, since the swelling might be anisotropic as the radial expansion is prohibited by the 3D printed shell. Fig. 4a-c show the microscope images of the ferrogel/magnet/ferrite core in the outer tube at different pH levels. The ferrogel dimensions (outlined by the white dashed box) increases with the increasing pH, as expected. The expanding ferrogel also pushes the ferrite core into the solenoid to modulate the inductance of the solenoid (the blue bar indicates the length of the ferrite rod outside of the solenoid and the red bar indicates the length of the ferrite rod inside of the solenoid). The inductance of the solenoid as a function of the core insertion length x is given as below,

$$L(x) = L_0 \cdot (1 + \mu_r \frac{x}{l}) \quad (1)$$

where L_0 is the inductance of the solenoid with the air-core, μ_r is the relative permeability of the ferrite core, and l is the total length of the solenoid. The resonance frequency of the sensor is then related to the core insertion length x by the equation below.

$$f = \frac{1}{2\pi\sqrt{LC}} = \frac{1}{2\pi\sqrt{C}}(L_0 \cdot (1 + \mu_r \frac{x}{l}))^{-1/2} \quad (2)$$

Since x << l, Taylor expansion of the equ. 2 yield equ. 3, where the shift in the resonant frequency is a linear function of the insertion length.

$$\Delta f = f - f_0 \approx f_0\left(1 - \frac{1}{2}\cdot \mu_r \frac{x}{l}\right) - f_0 = -\frac{f_0}{2}\cdot \mu_r \frac{x}{l} \quad (3)$$

The obtained swelling ratio in the axial direction and the insertion length of the ferrite rod is plotted in Fig. 4d and 4e, respectively. The swelling ratio of the ferrogel in the tube, also, was similar to the free swelling, in part, because the initial diameter of the ferrogel core was cut smaller than the tube diameter, allowing the radial expansion. We note that this is also important for the reversibility of the swelling as the clamped swelling tends to result in strain build-ups that compromises complete reversibility.

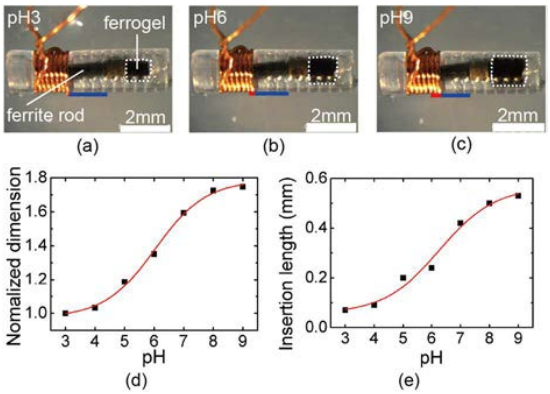

Figure 4. Swelling behavior of the ferrogel in the sensor (a-c) Microscope images of the ferrogel caged in the polymeric shell (the ferrogel is outlined by a dashed white line) at different pH. The color bar below the sensor indicates the length of the ferrite rod in (red) and out (blue) of the solenoid. (d) Swelling curve of the caged ferrogel. (e) Insertion length of the ferrite core to the solenoid as a function of pH

Wireless Biochemical Ferrogel Sensor Characterization

After establishing the ferrogel swelling and the ferrite core insertion into the solenoid under varying pH levels, we tested the sensor's resonance shift using a well-established phase-dip method [6] for wireless interrogation. The experimental setup is shown in Fig. 5a. The assembled sensor was placed in a 50 ml conical tube; a readout coil was wrapped around the tube and was connected to a network analyzer (ZND, Rohde & Schwarz, Germany). The pH response of the sensor was taken with the network analyzer after the ferrogel equilibrated after the solution exchange. The baseline corrected phase graphs for different pH showed clear pH dependent red-shift (Fig. 5b). We obtained the resonant frequency of the sensor by fitting Lorentzian curves to the baseline corrected phase graphs. The resulting resonant frequency of the wireless biochemical ferrogel sensor and the ferrite core insertion length are plotted as a function of pH (Fig. 5c). The ferrogel sensor's resonant frequency closely follows the core insertion length and the swelling curve, with a sharp transition pH of 6, consistent with the swelling data, obtained from the Boltzmann sigmoid curve fitting.

Finally, we carried out the wireless interrogation of the sensor using ultrasonic excitation of the RF signals (Fig.6a). We placed the sensor in a water tank under an ultrasonic transducer (TXH-1-75, Precision Acoustics, UK). The transducer was driven at its resonant frequency of 1 MHz in a burst mode using a function generator (AFG1022, Tektronix, USA) connected to an RF amplifier (240L, E&I, USA). A custom 3D printed holder was used to align the transducer with the wireless ferrogel sensor 8 cm apart corresponding to the focal length of the transducer. Under the ultrasonic pulses, the ultrasonic receiver outputs electrical power to the LC transponder, which emits the RF signal corresponding to its resonant frequency. The emitted RF signal was measured with a coil connected to an AD600-based broadband amplifier.

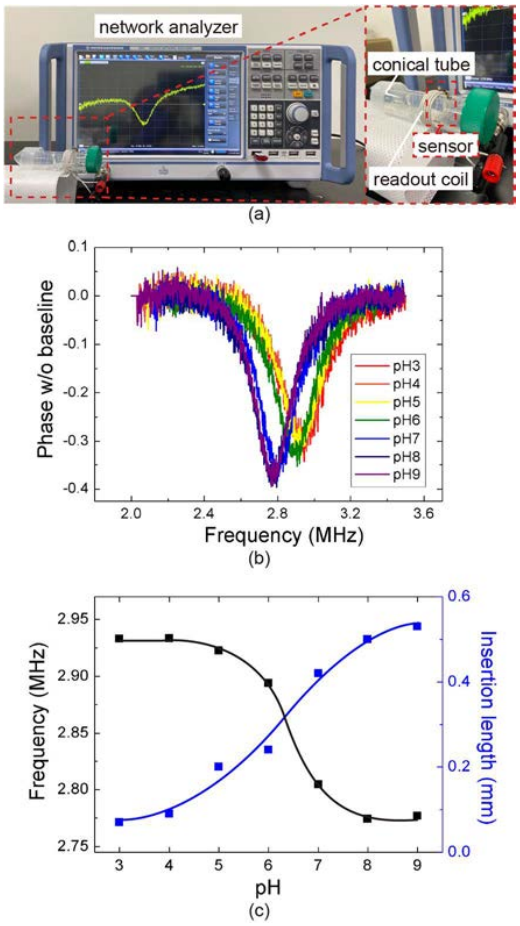

Figure 5. Verification of the wireless biochemical ferrogel sensor (a) Experimental setup (b) Baseline-corrected phase vs. frequency at different pH (c) Resonant frequency of the ferrogel sensor and the core insertion length as a function of pH showing a sharp transition at pH 6

A representative voltage trace when the voltage output of the piezoelectric receiver directly measured with an oscilloscope is shown in Fig. 6b. We observed the receiver voltage output (blue trace, Fig. 6b) with a time delay of 56 µs after the transducer input voltage was applied, which corresponds to 8 cm assuming 1450 m/s sound velocity in water. This time delay confirms that the origin of the voltage is from the applied ultrasound. With the appropriate selection of the ultrasonic intensity, we carried out the RF signal measurements under ultrasonic excitation.

Fig, 6c show representative time trace of the RF signal transmitted from the sensor's LC transponder. The observed time delay of 56 µs between the ultrasonic excitation (at t = 0 µs) and the received RF signal strongly indicates that the source of the RF signal is indeed from the ferrogel sensor. We also observed that the RF signal strength decays further away from the sensor. With the proper selection of the AD600 amplifier gain, we were able to detect RF signals 10 cm away from the sensor (Fig. 6c). Moreover, the FFT spectra of the received signal contains a frequency component closely matching the resonance of the LC transponder indicating that the sensor is capable of wireless pH sensing over a distance of 10 cm.

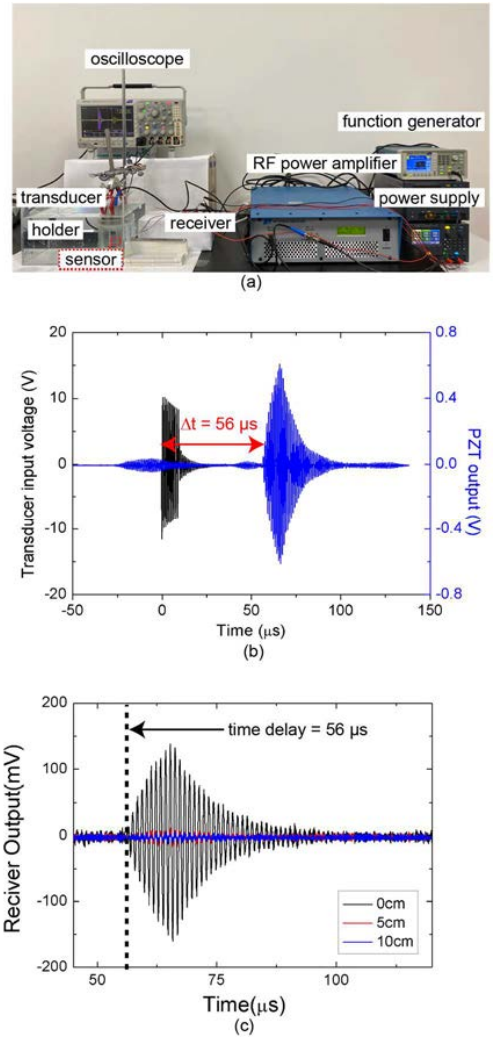

Figure 6. Wireless biochemical ferrogel sensor interrogation through ultrasonic excitation of RF signal (a) Experimental setup (b) Representative receiver output trace (c) Representative RF signal following the ultrasonic excitation at different distance between the sensor and the RF receiver coil

CONCLUSIONS

In this work, we developed and demonstrated a ferrogel based wireless pH sensor; the sensing element is composed of the assembly of ferrite rod/magnet/ferrogel that modulates the inductance of the solenoid and hence the resonant frequency of the LC transponder. The pH response of the ferrogel pH sensor closely matches the volumetric response of the pH sensitive hydrogel exhibiting Boltzmann sigmoid transition behavior from the ionization of the methacrylic acid. We also verified the RF transmission from the sensor under ultrasonic excitation with the sensing distance > 10 cm. Here we note, however, that we were not able to measure pH change in-situ using the ferrogel sensor due to the large volume of the water tank. Nevertheless, given the minute size of the sensor, < 10 mm in length and 2 mm in diameter, and the long working distance > 10 cm, the ferrogel pH sensor appears to be promising in wireless biochemical sensing applications with further development. Moreover, the sensor can be made to be sensitive to other biochemical parameters by changing the adopting different hydrogel composition.

ACKNOWLEDGEMENTS

This work was supported by the National Research Foundation of Korea (NRF) grant No. 2020R1C1C1006671.

REFERENCES

[1] W. L. Miller and R. J. Auchus, "The molecular biology, biochemistry, and physiology of human steroidogenesis and its disorders," *Endocr. Rev.*, vol. 32, no. 1, pp. 81–151, 2011.

[2] G. Li and D. Wen, "Wearable biochemical sensors for human health monitoring: sensing materials and manufacturing technologies," *J. Mater. Chem. B*, vol. 8, no. 16, pp. 3423–3436, 2020.

[3] S. M. George, S. Tandon, and B. Kandasubramanian, "Advancements in hydrogel-functionalized immunosensing platforms," *ACS omega*, vol. 5, no. 5, pp. 2060–2068, 2020.

[4] A. Matsumoto *et al.*, "Synthetic 'smart gel' provides glucose-responsive insulin delivery in diabetic mice," *Sci. Adv.*, vol. 3, no. 11, p. eaaq0723, 2017.

[5] J. Nam *et al.*, "A Hydrogel-Based Ultrasonic Backscattering Wireless Biochemical Sensing," *Front. Bioeng. Biotechnol.*, vol. 8, 2020.

[6] S. H. Song, J. H. Park, G. Chitnis, R. A. Siegel, and B. Ziaie, "A wireless chemical sensor featuring iron oxide nanoparticle-embedded hydrogels," *Sensors Actuators B Chem.*, vol. 193, pp. 925–930, 2014.

[7] H. Basaeri *et al.*, "Ultrasonically powered hydrogel-based wireless implantable glucose sensor," in *2016 IEEE SENSORS*, 2016, pp. 1–3.

[8] N. Kashyap, N. Kumar, and M. N. V. R. Kumar, "Hydrogels for pharmaceutical and biomedical applications," *Crit. Rev. Ther. Drug Carr. Syst.*, vol. 22, no. 2, 2005.

CONTACT

*S.H. Song, shsong.ee@sookmyung.ac.kr